

# Optical Activity from the Exciton Aharonov-Bohm Effect: A Floquet Engineering Approach

Kai Schwennicke<sup>1</sup> and Joel Yuen-Zhou<sup>1\*</sup>

<sup>1</sup>*Department of Chemistry and Biochemistry, University of California, San Diego, La  
Jolla, CA 92093, USA*

E-mail: joelyuen@ucsd.edu

## Abstract

Floquet engineering is a convenient strategy to induce nonequilibrium phenomena in molecular and solid-state systems, or to dramatically alter the physicochemical properties of matter, bypassing costly and time-consuming synthetic modifications. In this article, we investigate theoretically some interesting consequences of the fact that an originally achiral molecular system can exhibit nonzero circular dichroism (CD) when it is driven with elliptically polarized light. More specifically, we consider an isotropic ensemble of small cyclic molecular aggregates in solution whose local low-frequency vibrational modes are driven by an elliptically polarized continuous-wave infrared pump. We attribute the origin of a nonzero CD signal to time-reversal symmetry breaking due to an excitonic Aharonov-Bohm (AB) phase arising from a time-varying laser electric field, together with coherent interchromophoric exciton hopping. The obtained Floquet engineered excitonic AB phases are far more tunable than analogous magnetically-induced electronic AB phases in nanoscale rings, highlighting a virtually unexplored potential

that Floquet engineered AB phases have in the coherent control of molecular processes and simultaneously introducing new analogues of magneto-optical effects in molecular systems which bypass the use of strong magnetic fields.

## Introduction

Molecular enantiomers exhibit slightly different interactions with right and left-handed circular polarized (RCP, LCP) light fields. There are two important consequences of this effect: non-racemic samples exhibit finite circular dichroism (CD) (difference in absorption rate of RCP and LCP fields) and finite optical rotation (OR) (rotation of the plane of linearly polarized light). The phenomena of CD and OR are intimately related by Kramers-Kronig relations and are collectively known as “optical activity”<sup>1,2</sup>. CD and OR are well-established spectroscopic techniques to probe enantiomeric excess in chemical samples. Interestingly, optical activity is not restricted to samples involving chiral molecules, but can also arise in a material that interacts with a static magnetic field parallel to the propagation direction of light. To distinguish the optical activity due to a magnetic field from that due to the breakdown of molecular inversion symmetry, the former so-called magneto-optical (MO) effects are known as magnetic CD (MCD) and magnetic OR (MOR) or Faraday effect, respectively. MCD is an important spectroscopic technique that allows one to resolve electronic transitions in congested absorption bands<sup>3,4</sup>, while MOR is a phenomenon that is routinely exploited in the fabrication of optical devices such as isolators and circulators<sup>3,5,6</sup>.

The fundamental origin of MO effects is the breakdown of time-reversal symmetry (TRS). It is therefore reasonable that phenomena analogous to MO effects could arise from replacing a static magnetic field with time-varying electric fields; we shall hereafter term them pseudo-MO effects. In molecular spectroscopy, these phenomena have been long recognized since the pioneering work of Atkins and Miller<sup>7</sup>. More recently, within the context of topological photonics and nonreciprocal media, much attention has been directed towards exploiting time-varying modulation of material permittivities as a way to generate synthetic gauge

(“pseudo-magnetic”) fields, thereby circumventing magnetic field strengths that could be prohibitive in general experimental setups or difficult to integrate in optoelectronic devices. In fact, photonic versions of the Aharonov-Bohm (AB) effect<sup>8</sup> and quantum Hall systems<sup>9–11</sup> have been experimentally demonstrated. The the AB effect was observed for photons using a Ramsey-type interferometer<sup>12</sup>, while topologically protected photonic edge states were observed in a arrays constructed from optical ring resonators<sup>13</sup>. A hallmark of TRS breaking is the realization of AB phases that differ from 0 or  $\pi \bmod 2\pi$ . This version of AB phase is astutely realized in Reference 14 by driving resonators in adjacent unit cells so that there is a large phase lag between them, a feature that is facilitated by the relatively big mesoscopic lengthscales of the experimental system of interest. Thus, it is not obvious *a priori* whether such a strategy would be feasible in the recreation of pseudo-magnetic fields in molecular aggregates or in general nanoscale scenarios, especially considering the lengthscale mismatch between the typical interatomic or intermolecular distances and the optical wavelength of the driving field. However, as we shall show in the present article, such a mismatch can be compensated by invoking rings of coherently coupled anisotropic nanoscale molecular dipoles which simultaneously interact with an elliptically polarized laser field, such that different molecules interact with distinct linear polarizations of the laser and consequently pick up distinct phases from the light to break TRS. Our work follows a similar spirit to other theoretical proposals where an optically induced AB effect can be achieved in both electronic<sup>15</sup> and excitonic<sup>16,17</sup> nanoscopic ring structures by exploiting circularly polarized electric fields to break TRS. However, in these cases, the AB phase varies with field strength, while in our case the AB phase solely depends on the phase imprinted by the ellipticity of the field.

In this paper, we present a theoretical proof-of-principle of the possibility of inducing synthetic gauge fields in the excitonic degrees of freedom of small cyclic molecular aggregates. In particular, we design a setup consisting of an isotropic ensemble of molecular homotetramers, where each of the sites has an internal vibronic structure with low-frequency (e.g., vibra-

tional) transitions that are driven by a near-resonant electric field. Owing to the periodicity of the laser-driving, we employ Floquet theory<sup>18-20</sup> to calculate the spectral properties of the driven system according to a recently developed methodology<sup>21</sup>. These Floquet engineering concepts are complementary to efforts using strong magnetic fields to dramatically alter the vibronic structure and consequently the optical properties of molecular aggregates<sup>22</sup>, as well as to the design of topologically nontrivial phases in organic excitonic systems<sup>23</sup>. Although by no means a new technique, Floquet engineering is regaining interest in the development of materials with novel properties<sup>24</sup>, and in the proposal of using of Floquet engineering to influence both energy<sup>25</sup> and electron transfer<sup>26</sup> in molecular systems. In particular, our study highlights the simplicity with which large values of AB phases can be Floquet engineered with time varying electric fields in nanoscale systems (as shown below, with weak laser intensities), in contrast with the difficulties of deploying giant magnetic fields to generate similarly large values of AB phases. Hence, our results suggest much flexibility in the use of elliptically polarized light in the realization of excitonic AB phases in molecular systems, which could control a variety of charge and energy transfer processes in molecular aggregates or manipulate the spectroscopic properties of the latter. While excitonic AB phases that depend on the separation between electrons and holes have been studied in inorganic Wannier exciton systems<sup>27-31</sup>, similar phases in Frenkel organic exciton systems are far less explored (see Reference 23 for an example) and constitute an interesting frontier in physical chemistry.

## Theoretical Formalism

### Definition of excitonic model

The building block of our molecular aggregates is an anthracene molecule, depicted in Figure 1. We shall only be concerned with its  $S_0 \rightarrow S_1$  electronic transition (with 0-0' frequency  $\omega_e = 27,695 \text{ cm}^{-1}$ ) which is coupled to a low-frequency  $a_g$  mode ( $\omega_{vib} = 385 \text{ cm}^{-1}$ ); the

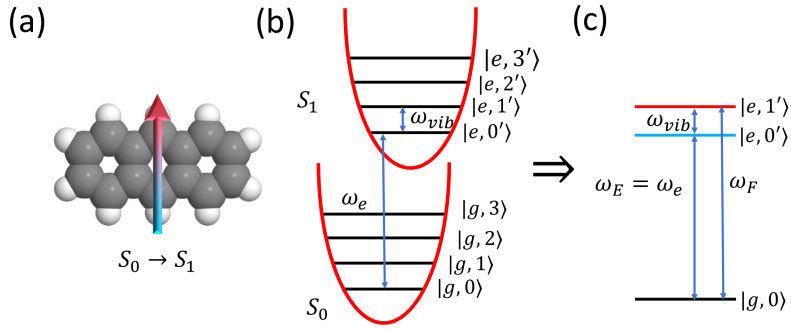


Figure 1: *Anthracene monomer*. (a) Molecular structure and dipole moment vector corresponding to the  $S_0 \rightarrow S_1$  transition. (b) Simplified displaced harmonic oscillator spectrum of anthracene along low-frequency vibrational mode ( $\omega_{vib} = 385 \text{ cm}^{-1}$ ). Here,  $\omega_e = 27,695 \text{ cm}^{-1}$  is the 0-0' electronic transition frequency and  $D = 0.31$  is the Huang-Rhys parameter for vibronic coupling. (c) In this work, we simplify the spectrum in (b) with a three-level model.

Huang-Rhys factor that characterizes the displacement of the  $S_1$  potential energy surface with respect to the  $S_0$  surface is  $D = 0.31$ <sup>32</sup>. These parameters were used in previous theoretical studies addressing how to control excitation-energy transfer by manipulating ultrafast vibrational dynamics in anthracene dimers<sup>33,34</sup>; the values were fit to experimental data involving vibrational coherences in anthracene dimers<sup>35</sup>. The weak vibronic coupling featured by this transition allows us to simplify the anthracene spectrum as an effective three-level system featuring ground  $|g, 0\rangle$  and excited  $|e, 0'\rangle$  electronic states with no phonons, and an excited  $|e, 1'\rangle$  electronic state with one phonon, where  $|g\rangle$  and  $|e\rangle$  denote  $S_0$  and  $S_1$  electronic states, and  $|\nu\rangle$  and  $|\nu'\rangle$  label vibrational eigenstates of the harmonic potentials corresponding to  $S_0$  and  $S_1$ , respectively (see Figure 1).

For simplicity, let us consider a homotetramer where the chromophores are located at the vertices of a square of side length  $a = 3.5 \text{ \AA}$ , mimicking values reported from the aforementioned ultrafast spectroscopy study<sup>35</sup> (see Figure 2). To unclutter notation, we introduce the following single-excitation basis:

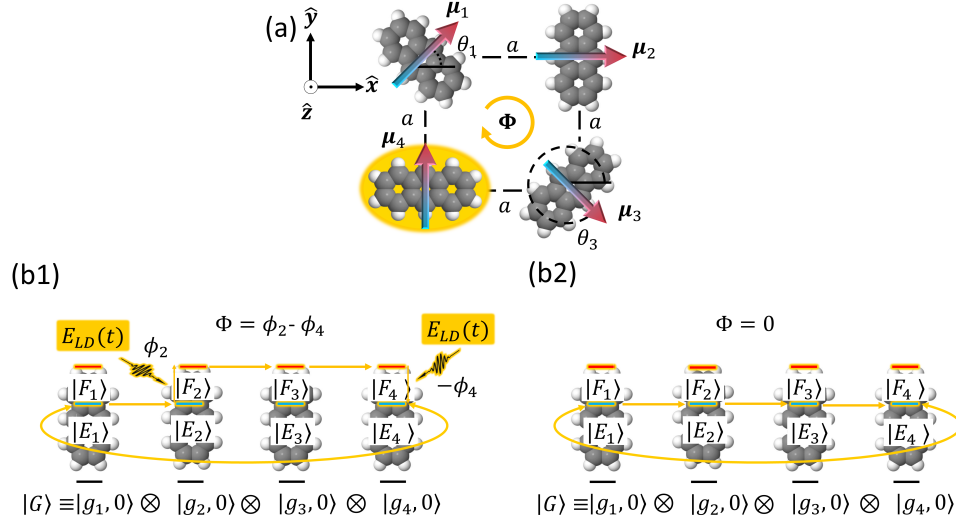


Figure 2: *Realization of excitonic Aharonov-Bohm (AB) effect in cyclic molecular aggregates via Floquet engineering with elliptically polarized light.* (a) Example geometry of an anthracene homotetramer where relative orientations ( $\theta_1, \theta_3$ ) of transition dipoles together with laser-driving induces an excitonic AB phase  $\Phi$ . The anthracene monomers are equidistantly placed at a distance  $a$  from their neighbors forming a square. (b) Schematic illustration of the mechanism whereby Floquet engineering induces excitonic AB phases. The elliptically polarized field  $E_{LD}(t)$  drives the  $|E_i\rangle \rightarrow |F_i\rangle$  low-frequency vibrational transition (vertical yellow arrows). Horizontal yellow arrows denote excitonic couplings mediated by electrostatic interactions. In (b1), excitation of the first chromophore at  $|E_1\rangle$  is resonantly transferred to the second chromophore  $|E_2\rangle$  via a dipolar coupling. Next, the laser promotes the  $|E_2\rangle \rightarrow |F_2\rangle$  vibrational excitation, “dialing” phase  $\phi_2$  onto that transition. Subsequent excitation transfer  $|F_2\rangle \rightarrow |F_3\rangle \rightarrow |F_4\rangle$  occurs via resonant dipolar couplings, after which the laser promotes the  $|F_4\rangle \rightarrow |E_4\rangle$  vibrational emission, dialing phase  $-\phi_4$  onto that transition. Finally another step of resonant dipole-mediated excitation transfer  $|E_4\rangle \rightarrow |E_1\rangle$  closes the loop, yielding an AB phase  $\Phi = \phi_2 - \phi_4$ .  $\Phi \neq n\pi$  for integer  $n$  signals time-reversal symmetry breaking. Meanwhile (b2) illustrates a pathway mediated by electrostatic interactions (and no influence from laser-driving) that does not result in nontrivial AB phase.

$$|G\rangle = \prod_{i=1}^4 |g_i, 0_i\rangle, \quad (1a)$$

$$|E_j\rangle = |e_j, 0'_j\rangle \prod_{i \neq j}^4 |g_i, 0_i\rangle, \quad (1b)$$

$$|F_j\rangle = |e_j, 1'_j\rangle \prod_{i \neq j}^4 |g_i, 0_i\rangle. \quad (1c)$$

The excitonic Hamiltonian of the homotetramer reads ( $\hbar = 1$ )

$$H_T = \sum_{i=1}^4 \left( \omega_E |E_i\rangle \langle E_i| + \omega_F |F_i\rangle \langle F_i| \right) + \sum_{\langle ij \rangle} \left[ (J_{E_i, E_j} |E_i\rangle \langle E_j| + J_{E_i, F_j} |E_i\rangle \langle F_j| + J_{F_i, F_j} |F_i\rangle \langle F_j|) + \text{h.c.} \right], \quad (2)$$

where the sum over  $\langle ij \rangle$  assumes only nearest-neighbor couplings. Here  $\omega_E = \omega_e$  and  $\omega_F = \omega_e + \omega_{vib} = 28,080 \text{ cm}^{-1}$ , and  $J_{\alpha\beta} = J_{\beta\alpha}$  are the electrostatic couplings between excitonic states  $|\alpha\rangle$  and  $|\beta\rangle$ , which are calculated assuming the Condon approximation<sup>36,37</sup>, e.g.

$$J_{E_i, F_j} = \langle e_i g_j | H_T | g_i e_j \rangle \langle 0'_i | 0_i \rangle \langle 0_j | 1'_j \rangle,$$

where

$$\langle e_i g_j | H_T | g_i e_j \rangle = \eta \frac{(\hat{\boldsymbol{\mu}}_i \cdot \hat{\boldsymbol{\mu}}_j) - 3(\hat{\boldsymbol{\mu}}_i \cdot \hat{\mathbf{r}}_{ij})(\hat{\boldsymbol{\mu}}_j \cdot \hat{\mathbf{r}}_{ij})}{a^3}$$

is approximated as the classical dipole-dipole interaction, with  $\hat{\boldsymbol{\mu}}_i$  being the unit vector of the electronic transition dipole moment for the  $S_0 \rightarrow S_1$  transition for the  $i$ -th chromophore and  $\hat{\mathbf{r}}_{ij}$  being the unit vector that connects chromophores  $i$  and  $j$ . The value  $\eta = 982 \text{ cm}^{-1} \text{ \AA}^3$  has been invoked to account for the effects of transition dipole magnitudes as well as the index of refraction of the surrounding medium, so that the dipolar coupling between parallel anthracene molecules is  $\langle e_i g_j | H_T | g_i e_j \rangle = \frac{\eta}{a^3} = 22.9 \text{ cm}^{-1}$ <sup>33,34</sup>, a value that

is consistent with quantum beat data in ultrafast spectroscopy experiments<sup>35</sup>. The scalar  $|\langle n'_i|0_i\rangle|^2 = \exp[-D]\frac{D^n}{n!}$  is the relevant Franck-Condon factor<sup>36</sup>. In this work, we fix the orientations of  $\boldsymbol{\mu}_2$  and  $\boldsymbol{\mu}_4$  to be along the  $\hat{\boldsymbol{x}}$  and  $\hat{\boldsymbol{y}}$  axes, respectively, in the molecular aggregate frame, while we vary the orientations of  $\boldsymbol{\mu}_1$  and  $\boldsymbol{\mu}_3$  at angles  $\theta_1$  and  $\theta_3$  (Figure 2a shows  $\theta_1 = 45^0$  and  $\theta_3 = 315^0$ ). For simplicity, we ignore out-of-plane dipole orientations; this is not a necessary condition and could be easily lifted if chemical synthesis favors other geometries. The excitonic transition dipole moments from the ground state,  $|G\rangle$ , are  $\boldsymbol{\mu}_{E_iG} = \langle E_i|\boldsymbol{\mu}|G\rangle = \langle e_i, 0'_i|\boldsymbol{\mu}|g_i, 0_i\rangle$  and  $\boldsymbol{\mu}_{F_iG} = \langle F_i|\boldsymbol{\mu}|G\rangle = \langle e_i, 1'_i|\boldsymbol{\mu}|g_i, 0_i\rangle$ . In our calculations we take  $\langle e_i, 0'_i|\boldsymbol{\mu}|g_i, 0_i\rangle = 0.90$  Debye and  $\langle e_i, 1'_i|\boldsymbol{\mu}|g_i, 0_i\rangle = 0.74$  Debye, values which are consistent with experiments<sup>35</sup>.

Given that  $J_{\alpha\beta} \ll \omega_{vib}$ , the exciton eigenstates of  $H_T$  consist of two bands centered at  $\omega_E$  and  $\omega_F$ , respectively, with bandwidths  $\sim 2\max|J_{E_iE_j}|$ ,  $\sim 2\max|J_{F_iF_j}|$ . Figure 3 shows the absorption spectrum of an isotropically averaged collection of homotetramers. Notice that due to different Franck-Condon overlaps, the splitting of the band at  $\omega_F$  is narrower than that at  $\omega_E$ . Note, there are multiple vibronic eigenstates whose symmetries result in net zero transition dipole moments; that is, they are dark with respect to UV-visible light in the absence of laser-driving. Accordingly, these states cannot be observed using absorption spectroscopy, which is why there are fewer peaks in the spectrum than the number of possible eigenstates of  $H_T$ .

## Floquet theory for laser-driving

The aforementioned two bands can be mixed upon introduction of a driving laser; the new Hamiltonian is time-dependent and reads

$$H_{LD}(t) = H_T - \sum_{i=1}^4 (\boldsymbol{\mu}_{E_iF_i} \cdot \mathbf{E}_{LD}(t)|E_i\rangle\langle F_i| + \text{h.c.}), \quad (3)$$



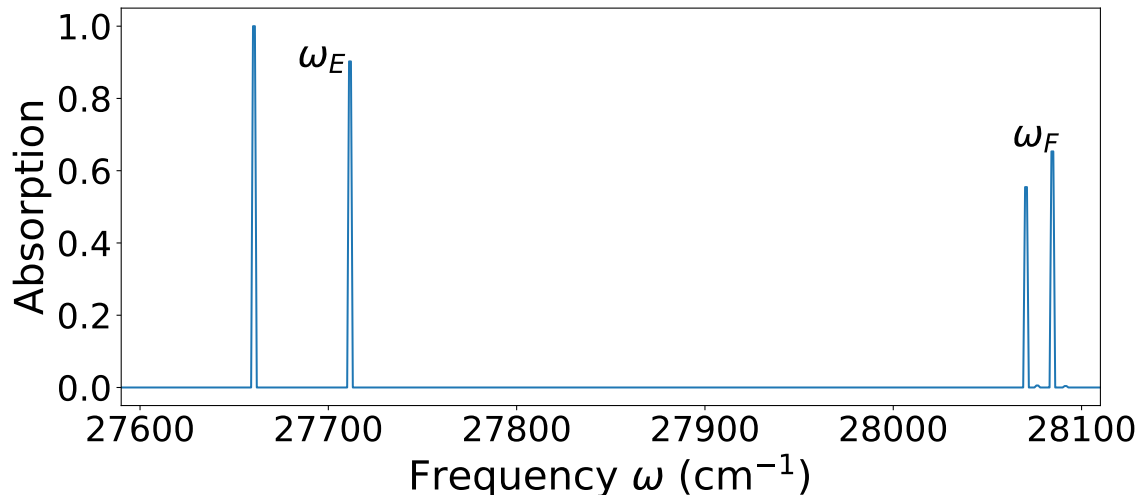


Figure 3: *Absorption spectrum of an isotropic solution of excitonic homotetramers.* It can be approximately understood as consisting of two bands of transitions corresponding to coherent combinations of 0-0' transitions (centered at  $\omega_E$ ) and 0-1' transitions (centered at  $\omega_F$ ) respectively. The splitting of each of these bands is due to resonant exciton hopping between molecules, and correspond to  $\sim 2\max|J_{E_i E_j}|$  and  $\sim 2\max|J_{F_i F_j}|$ , respectively.

where we have introduced an infrared (IR) field at a frequency  $\Omega = \omega_{vib} + \delta$  that is slightly detuned from the  $E_i \rightarrow F_i$  vibrational transitions by  $\delta$ :

$$\mathbf{E}_{LD}(t) = \frac{E_{LD}^0}{\sqrt{2}} [\hat{x} \cos(\Omega t + \phi_x) + \hat{y} \cos(\Omega t + \phi_y)].$$

The detuning  $\delta$  allows us to ignore resonant pumping of vibrational transitions in the ground state (Figure 1b) so that the three-level approximation per molecule (Figure 1c) is justified. The phases  $\phi_x$  and  $\phi_y$  will play an important role below. The relevant transition dipole moments to the laser-driving are  $\boldsymbol{\mu}_{F_i E_i} = \langle F_i | \boldsymbol{\mu} | E_i \rangle = \langle e_i, 1'_i | \boldsymbol{\mu} | e_i, 0'_i \rangle$  and we take  $|\boldsymbol{\mu}_{F_i E_i}| = 0.15$  Debye, which is a reasonable value for IR molecular vibrational excitations<sup>38</sup>.

For completeness, we shall now lay out the Floquet theory<sup>18-20</sup> utilized to address the problem in question. The Hamiltonian  $H_{LD}(t)$  is periodic in time with period  $T = 2\pi/\Omega$  such that  $H_{LD}(t+T) = H_{LD}(t)$ . The solutions to the time dependent Schrödinger equation

(TDSE)

$$i \frac{d}{dt} |\Psi(t)\rangle = H_{LD}(t) |\Psi(t)\rangle$$

can be written in the Floquet state basis  $|\Psi(t)\rangle = \sum_{\lambda} C_{\lambda} |\psi_{\lambda}(t)\rangle$  where

$$|\psi_{\lambda}(t)\rangle = e^{-i\varepsilon_{\lambda}t} |\phi_{\lambda}(t)\rangle. \quad (4)$$

The Floquet modes can be spectrally decomposed in the single (molecular) excitation basis,  $\alpha \in \{G, E_i, F_i\}$  where  $i \in \{1, 2, 3, 4\}$ , introduced in Eq. (1),

$$|\phi_{\lambda}(t)\rangle = \sum_{\alpha} |\alpha\rangle \langle \alpha | \phi_{\lambda}(t)\rangle, \quad (5)$$

and are periodic in time with period  $T$ . Furthermore, they are eigenfunctions of the Floquet Hamiltonian

$$H_F |\phi_{\lambda}(t)\rangle = \left[ H_{LD}(t) - i \frac{d}{dt} \right] |\phi_{\lambda}(t)\rangle = \varepsilon_{\lambda} |\phi_{\lambda}(t)\rangle, \quad (6)$$

where the eigenvalues  $\{\varepsilon_{\lambda}\}$  are known as quasi-energies. Since  $|\phi_{\lambda}(t)\rangle$  and  $H_{LD}(t)$  are time-periodic, we can write Eqs. (3) and (5) in terms of their Fourier components:

$$|\phi_{\lambda}(t)\rangle = \sum_{\alpha} \sum_{n=-\infty}^{\infty} |\alpha\rangle \langle \alpha | \phi_{\lambda}^{(n)}\rangle e^{in\Omega t}, \quad (7a)$$

$$\langle \alpha | H_{LD}(t) | \beta \rangle = \sum_{n=-\infty}^{\infty} H_{LD,\alpha\beta}^{(n)} e^{in\Omega t}, \quad (7b)$$

where  $H_{LD,\alpha\beta}^{(n)} = \frac{1}{T} \int_0^T dt \langle \alpha | H_{LD}(t) | \beta \rangle e^{-in\Omega t}$ . By substituting Eqs. (7a) and (7b) into Eq. (6), multiplying both sides of the resulting equation by  $\exp(-ik\Omega t)$ , and taking a time-integral over one period  $T$ , we obtain

$$\sum_{\beta n} H_{F\alpha\beta}^{(k-n)} \langle \beta | \phi_\lambda^{(n)} \rangle = \varepsilon_\lambda \langle \alpha | \phi_\lambda^{(k)} \rangle, \quad (8a)$$

$$H_{F\alpha\beta}^{(k-n)} = H_{LD,\alpha\beta}^{(k-n)} + n\Omega \delta_{\alpha\beta} \delta_{kn}. \quad (8b)$$

At this point, we augment the Hilbert space from  $|\alpha\rangle$  to  $|\alpha\rangle \otimes |t\rangle$ , where  $\langle t | \phi_\lambda \rangle = |\phi_\lambda(t)\rangle$ , and introduce the Fourier basis  $\{|n\rangle\}$  where  $\langle n | \phi_\lambda \rangle \equiv |\phi_\lambda^{(n)}\rangle$ ,  $\langle t | n \rangle = e^{in\Omega t}$ ,  $|\alpha, n\rangle \equiv |\alpha\rangle |n\rangle$ , and  $\langle \alpha, k | H_F | \beta, n \rangle \equiv H_{F\alpha\beta}^{(k-n)}$ , rendering the eigenvalue problem into the following form:

$$H_F |\phi_\lambda\rangle = \left[ H_F^{(0)} + H_F^{(1)} \right] |\phi_\lambda\rangle = \varepsilon_\lambda |\phi_\lambda\rangle, \quad (9a)$$

$$H_F^{(0)} = \sum_{n=-\infty}^{\infty} \left\{ \sum_{i=1}^4 \left[ (\omega_E + n\Omega) |E_i, n\rangle \langle E_i, n| + (\omega_F + n\Omega) |F_i, n\rangle \langle F_i, n| \right] + n\Omega |G, n\rangle \langle G, n| \right. \\ \left. + \sum_{\langle ij \rangle} \left[ (J_{E_i, E_j} |E_i, n\rangle \langle E_j, n| + J_{E_i, F_j} |E_i, n\rangle \langle F_j, n| + J_{F_i, F_j} |F_i, n\rangle \langle F_j, n|) + \text{h.c.} \right] \right\}, \quad (9b)$$

$$H_F^{(1)} = -\frac{E_{LD}^0}{\sqrt{2}} \sum_{n=-\infty}^{\infty} \left\{ \sum_{i=1}^4 \sum_{q=\hat{x}, \hat{y}} \left[ \mu_{E_i F_i}^q (e^{i\phi_q} |E_i, n\rangle \langle F_i, n+1| + e^{-i\phi_q} |E_i, n+1\rangle \langle F_i, n|) + \text{h.c.} \right] \right\}. \quad (9c)$$

An intuitive interpretation of this basis, which was originally presented by Shirley<sup>18</sup>, comes from associating  $n$  to the number of quanta present in the laser-driving mode; e.g.,  $|E_1, 3\rangle$  would refer to the state were the exciton corresponds to the 0-0' transition in first chromophore while the field contains three photons. Following this interpretation, Eq. (9b) denotes that intermolecular interactions between excitonic states preserve photon number, while Eq. (9c) shows that the driving field couples states  $|E_i\rangle, |F_i\rangle$  by either absorbing or

emitting a photon. To gain further insight, we consider the limit where

$$|J_{E_i F_j}|, |\boldsymbol{\mu}_{LD} \cdot \mathbf{E}_{LD}(t)| \ll \Omega, \quad (10)$$

so that we can apply the rotating-wave approximation (RWA) to drop highly off-resonant terms; Eqs. (9b) and (9c) can then be reduced to

$$\begin{aligned} H_F^{(0)} \approx & \sum_{n=-\infty}^{\infty} \left\{ \sum_{i=1}^4 \left[ (\omega_E + n\Omega) |E_i, n\rangle \langle E_i, n| + (\omega_F + n\Omega) |F_i, n\rangle \langle F_i, n| \right] + n\Omega |G, n\rangle \langle G, n| \right. \\ & \left. + \sum_{\langle ij \rangle} \left[ (J_{E_i, E_j} |E_i, n\rangle \langle E_j, n| + J_{F_i, F_j} |F_i, n\rangle \langle F_j, n|) + \text{h.c.} \right] \right\} \end{aligned} \quad (11a)$$

$$H_F^{(1)} \approx -\frac{E_{LD}^0}{\sqrt{2}} \sum_{n=-\infty}^{\infty} \left\{ \sum_{i=1, q}^4 \left[ \mu_{E_i F_i}^q e^{-i\phi_q} |E_i, n+1\rangle \langle F_i, n| + \text{h.c.} \right] \right\}. \quad (11b)$$

The RWA invokes a physically intuitive constraint: the laser-driving intensity is weak enough that it can only induce the  $|E_i\rangle \rightarrow |F_i\rangle$  transition if the exciton absorbs a photon from the field. Furthermore, the RWA block-diagonalizes Eq. (9a) so that  $H_F \approx \sum_n (h_{F,n} + h_{G,n})$  where the  $n$ -th blocks  $h_{G,n}$  and  $h_{F,n}$  are defined as:

$$h_{G,n} = n\Omega |G, n\rangle \langle G, n|, \quad (12a)$$

$$\begin{aligned} h_{F,n} = & \sum_{i=1}^4 \left[ (\omega_E + (n+1)\Omega) |E_i, n+1\rangle \langle E_i, n+1| + (\omega_F + n\Omega) |F_i, n\rangle \langle F_i, n| \right] \\ & + \sum_{\langle ij \rangle} \left[ (J_{E_i, E_j} |E_i, n+1\rangle \langle E_j, n+1| + J_{F_i, F_j} |F_i, n\rangle \langle F_j, n|) + \text{h.c.} \right] \\ & - \frac{E_{LD}^0}{\sqrt{2}} \sum_{i=1, q}^4 \left[ \mu_{E_i F_i}^q e^{-i\phi_q} |E_i, n+1\rangle \langle F_i, n| + \text{h.c.} \right]. \end{aligned} \quad (12b)$$

Note that the Floquet states  $\{|\psi_\lambda(t)\rangle\}$  are uniquely characterized by the quasi-energies  $\varepsilon_\lambda \bmod \Omega$ <sup>18,20</sup>; therefore, within the RWA, we only need to diagonalize one  $h_{F,n}$  block and

one  $h_{G,n}$  block to find a finite set of Floquet modes  $\{|\phi_\lambda\rangle\}$  to construct the Floquet state basis  $\{|\psi_\lambda(t)\rangle\}$ . We should note that Eq. (12b) resembles a lattice Hamiltonian where the quantum degrees of freedom are influenced by a gauge field  $\vec{\mathbf{A}}(\mathbf{r})$ <sup>39</sup>, where  $\phi_q = \int \vec{\mathbf{A}}(\mathbf{r}) \cdot d\mathbf{r}$ . Typically, the latter arises from a magnetic field coupling to movable charges, resulting in AB phases; in our case, we shall see that the gauge field is a result of the elliptically polarized laser, which can be thought of as a pseudo-magnetic field.

## Calculation of circular dichroism spectrum

To calculate the CD signal of the laser-driven system, we invoke the formalism developed in Reference 21. We compute the rates of absorption  $W_\pm$  due to weak-intensity continuous-wave circularly polarized probe laser fields at UV-visible frequency  $\omega$ ,

$$\mathbf{E}_{P\pm}(\omega, t) = \frac{E_P^0}{\sqrt{2}}(\hat{\mathbf{x}} \cos \omega t \pm \hat{\mathbf{y}} \sin \omega t).$$

The CD response at each frequency  $\omega$  is defined as the difference  $\delta W(\omega) = W_+(\omega) - W_-(\omega)$  in the rates due to RCP and LCP light,

$$\delta W(\omega) = -|E_p^0|^2 \pi \text{Im} \left[ \sum_{\lambda, \alpha, \beta} \sum_{n=-\infty}^{\infty} \mu_{\alpha G}^y \langle \phi_\lambda | \alpha n \rangle \mu_{G\beta}^x \langle \beta n | \phi_\lambda \rangle \delta(\varepsilon_\lambda - n\Omega - \omega) \right]. \quad (13)$$

Here  $\varepsilon_\lambda - n\Omega$  denotes the  $|Gn\rangle \rightarrow |\phi_\lambda\rangle$  transition energy, where  $|\phi_\lambda\rangle$  is an eigenstate of  $h_{F,1}$  or  $h_{G,1}$  (see Eqs. (12a), (12b)) with eigenvalue  $\varepsilon_\lambda$ , and  $\omega$  is the energy absorbed from the probe. Note that  $\mu_{GG} = 0$  and, due to the RWA,  $h_{F,1}$  only couples the states  $|E_i, 2\rangle$  and  $|F_i, 1\rangle$ . Therefore,  $\langle \alpha, n | \phi_\lambda \rangle \neq 0$  only for  $n = 1, 2$ , which results in Eq. (13) being simplified to

$$\delta W(\omega) = -|E_p^0|^2 \pi \text{Im} \left[ \sum_{\lambda} \sum_{ij} \left\{ \mu_{E_i G}^y \langle \phi_\lambda | E_i 2 \rangle \mu_{G E_j}^x \langle E_j 2 | \phi_\lambda \rangle \delta(\varepsilon_\lambda - 2\Omega - \omega) \right. \right. \\ \left. \left. + \mu_{F_i G}^y \langle \phi_\lambda | F_i 1 \rangle \mu_{G F_j}^x \langle F_j 1 | \phi_\lambda \rangle \delta(\varepsilon_\lambda - \Omega - \omega) \right\} \right]. \quad (14)$$

Eq. (14) corresponds to the CD for a single homotetramer of fixed orientation. Since we are interested in an isotropic film or solution of such aggregates, we must take an average of  $\delta W(\omega)$  over different orientations of the tetramer with respect to the incident light  $\mathbf{k}$  vector,

$$\langle \delta W(\omega) \rangle = \frac{1}{8\pi^2} \int_0^{2\pi} \int_0^{2\pi} \int_0^\pi d\chi d\psi d\theta W(\omega; \chi, \psi, \theta) \sin\theta, \quad (15)$$

where we have explicitly written  $\delta W(\omega) = \delta W(\omega; \chi, \psi, \theta)$  to express the fact that the CD for each aggregate is a function of its orientation, defined by Tait-Bryan angles  $\chi, \psi, \theta$ <sup>40</sup> (see Figure 4). Notice that unlike with perturbative spectroscopy<sup>41</sup>, we cannot analytically carry out this average given that  $h_{F,1}$  is a function itself of  $\chi, \psi, \theta$ , as each orientation experiences a different driving due to its different dipole projections with the IR laser. Hence, we compute the isotropically averaged CD spectrum in Eq. (15) via Monte Carlo integration (see Supplementary Information).

## Results and Discussion

### Excitonic AB phases

To illustrate the nontrivial effects produced by Floquet engineering, we now consider coherent pathways due to the various terms in Eq. (12). In particular, we are interested in cyclic ones, namely, those which begin and end in the same state. For concreteness, let us focus on the pathway depicted in Figure 2b1. Excitation of the first chromophore at  $|E_1\rangle$  is resonantly transferred to the second chromophore  $|E_2\rangle$  via dipolar coupling. Next, the elliptically polarized driving laser promotes the  $|E_2\rangle \rightarrow |F_2\rangle$  vibrational excitation, imprinting a nontrivial phase  $\phi_2$  onto that transition. Subsequent excitation transfer via dipolar coupling  $|F_2\rangle \rightarrow |F_3\rangle \rightarrow |F_4\rangle$  is followed by a laser-induced vibrational de-excitation  $|F_4\rangle \rightarrow |E_4\rangle$ , which imprints yet another nontrivial phase  $\phi_4$ ; the pathway is closed by another dipolar coupling  $|E_4\rangle \rightarrow |E_1\rangle$ . To make these statements more precise, let us define the Wilson loop<sup>42</sup> corresponding to this pathway:

$$\begin{aligned}
\mathcal{W} &= \langle E_1 n | h_{F,n} | E_4 n + 1 \rangle \langle E_4 n + 1 | h_{F,n} | F_4 n \rangle \langle F_4 n | h_{F,n} | F_3 n \rangle \\
&\times \langle F_3 n | h_{F,n} | F_2 n \rangle \langle F_2 n | h_{F,n} | E_2 n + 1 \rangle \langle E_2 n + 1 | h_{F,n} | E_1 n + 1 \rangle \\
&= J_{E_1 E_2} \left( \sum_{q=\hat{x}, \hat{y}} \frac{E_{LD}^0 \mu_{E_2 F_2}^q}{\sqrt{2}} e^{i\phi_q} \right) J_{F_2 F_3} \\
&\times J_{F_3 F_4} \left( \sum_{q=\hat{x}, \hat{y}} \frac{E_{LD}^0 \mu_{E_2 F_2}^q}{\sqrt{2}} e^{-i\phi_q} \right) J_{E_4 E_1}.
\end{aligned}$$

If we define

$$\begin{aligned}
\phi_2 &= \arg \left[ J_{E_1 E_2} \left( \sum_{q=\hat{x}, \hat{y}} \frac{E_{LD}^0 \mu_{E_2 F_2}^q}{\sqrt{2}} e^{i\phi_q} \right) J_{F_2 F_3} \right], \\
\phi_4 &= -\arg \left[ J_{F_3 F_4} \left( \sum_{q=\hat{x}, \hat{y}} \frac{E_{LD}^0 \mu_{E_2 F_2}^q}{\sqrt{2}} e^{-i\phi_q} \right) J_{E_4 E_1} \right],
\end{aligned}$$

the excitonic AB phase corresponding to this pathway is equal to  $\Phi = \arg(W) = \phi_2 - \phi_4$ . To gain further intuition on the types of transition dipole arrangements that lead to substantial values of  $\Phi$ , let us consider the configuration in Figure 2a, where the dipoles in chromophores 2 and 4 are aligned along  $\hat{x}$  and  $\hat{y}$  respectively, and the only positive dipolar couplings within our gauge convention is  $J_{F_2 F_3}$ ; then,  $\phi_2 = \phi_x + \pi$  and  $\phi_4 = -\phi_y - 2\pi = -\phi_y$ , so that the phases of the elliptically polarized field are explicitly imprinted in the resulting excitonic AB phase

$$\Phi = \arg(\mathcal{W}) = \phi_x - \phi_y + \pi = \Delta\phi + \pi.$$

A few comments are pertinent at this point. When  $\Delta\phi = 0 \bmod \pi$ , the driving laser corresponds to linearly polarized light and the AB phase  $\Phi = 0, \pi$  is trivial; this is expected as TRS is preserved. However, when  $\Delta\phi \neq 0 \bmod \pi$ , the driving laser corresponds to elliptically polarized light, leading to a nontrivial AB phase  $\Phi \neq 0, \pi$  ( $\Delta\phi = \frac{\pi}{2} \bmod \pi$  corresponds to the

special case of circular polarization) that signals TRS breaking. Hence, our design crucially depends on chromophores 2 and 4 obtaining different phases  $\phi_x$  and  $\phi_y$  from the laser-driving; to maximize this difference, they are placed perpendicular to one another. However, the production of a nontrivial AB phase relies also on having coherent dipolar couplings throughout the aggregate that yield a nonzero Wilson loop. To ensure that chromophores 2 and 4 are coupled, chromophores 1 and 3 are positioned along optimal orientations  $\frac{\hat{x} \pm \hat{y}}{\sqrt{2}}$  so that the exciton hoppings are enough to ensure large coherent couplings throughout the cycle. It follows that to realize an exciton AB phase  $\Phi = \frac{\pi}{2}$ , one simply needs to set  $\Delta\phi = -\frac{\pi}{2}$ , corresponding to right circularly polarized light. At this point, it is worth highlighting that this excitonic AB phase is independent of laser intensity so long as the RWA is a good approximation. This should be contrasted with the magnitudes of the magnetic fields used to generate an AB phase  $\Phi = \frac{\pi}{2}$  in a nanoscale ring supporting electronic currents. In fact, considering a putative loop of the same area  $a^2$  as our molecular aggregate,  $\Phi = \frac{eBa^2}{h}$  would require  $B = 8400$  Tesla (an intensity that is only feasible at present in restricted places such as white dwarfs!<sup>43</sup>). This remark implies that it should be substantially easier to realize AB phases in nanoscale systems by employing Floquet engineering via time-varying laser electric fields over giant static magnetic fields. Thus, these versatile Floquet engineered AB phases could open doors to new ways of coherently controlling excitonic processes in molecules and nanomaterials.

Our proposal to induce AB phases via Floquet engineering is heavily influenced by Reference 14, where the authors suggest the periodic modulation of permittivities in arrays of coherently coupled resonators to generate pseudo-magnetic fields. Crucial to their setup is a well-crafted spatial distribution of modulation phases which is locally controlled with electrical circuit elements. This local control of phases is possible in mesoscopic systems but much harder to realize in the nanoscale. In fact, one could be tempted to think that light-matter interaction is ineffective in doing so, given the mismatch between the lengthscale of light and molecules. However, as we show in our example above, we achieve the distribution of



modulation phases by exploiting (a) the phase lag between the  $\hat{x}$  and  $\hat{y}$  components of the electric field of elliptically polarized laser light and (b) by designing rings of coherently coupled molecular dipoles where different sites feature orientations that interact with different polarizations of the laser light.

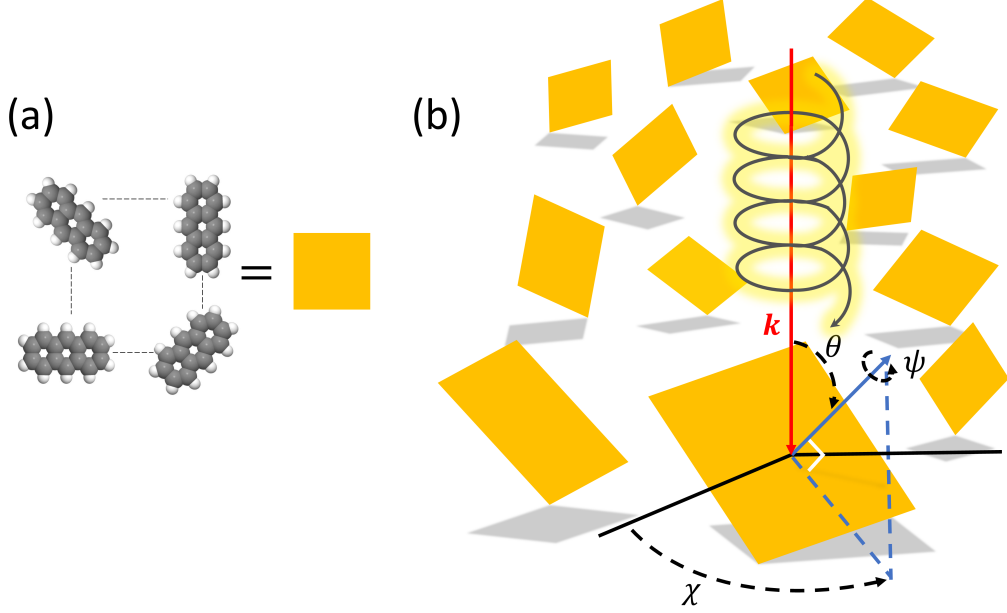


Figure 4: (a) Excitonic homotetramer unit. (b) Depiction of isotropic ensemble of homotetramers; calculation of circular dichroism (CD) involves averaging over orientations  $\chi, \theta, \psi$  with respect to the  $\mathbf{k}$  vector of the incident beam. Here, the normal vector to the molecular aggregate plane (blue arrow) is uniquely defined by the polar coordinates  $\theta$  and  $\chi$ , while  $\psi$  is the angle of rotation of the aggregate about the aforementioned vector. Note that the ellipticity of the incident beam is not represented to scale with respect to the molecular aggregates.

## Features of the CD spectrum

To test the effects of TRS breaking due to nontrivial excitonic AB phases, Figure 5 shows the isotropic averaged CD spectrum  $\langle \delta W(\omega) \rangle$  normalized to the maximum absorption of the isotropic solution in the absence of driving. For our simulations, we use  $E_{LD}^0 = 2.7 \times 10^8 \frac{V}{m}$ , which is a standard value utilized in Floquet engineering experiments with inorganic

semiconductors<sup>44</sup>, and take  $\delta = -0.1\omega_{vib}$ . With these parameters we obtain  $\frac{|\boldsymbol{\mu}_{LD} \cdot \mathbf{E}_{LD}(t)|}{\Omega} = 0.02$ , which satisfies the requirement of Eq. (10) above. As expected, when  $\Delta\phi = 0, \pi$ ,  $\langle\delta W(\omega)\rangle$  vanishes for all  $\omega$ : TRS is preserved under linearly polarized light driving. However, arbitrary elliptically polarized fields ( $\Delta\phi \neq 0, \pi$ ) give rise to nonzero CD, where a clear pattern of sign switches occurs at the TRS points. Notice that despite the laser-driving being weak in comparison to its carrier frequency,  $|\boldsymbol{\mu}_{LD} \cdot \mathbf{E}_{LD}(t)| \ll \Omega$  (see Eq. (10)), the small shifts in peak frequencies in Figure 3 give rise to substantial CD signals, just as in MCD, where moderate values of magnetic fields can easily dissect congested spectra<sup>3,4</sup>. Also note that the maximum absolute value of  $\langle\delta W(\omega)\rangle$  occurs at  $\Delta\phi = \frac{\pi}{2}, \frac{3\pi}{2}$ , which corresponds to circularly polarized light. Based on the mechanism outlined in the previous subsection (see also Figures 2a, b), we attribute this symmetry to the fact that in our homotetramer, the dipoles are all of the same magnitude.

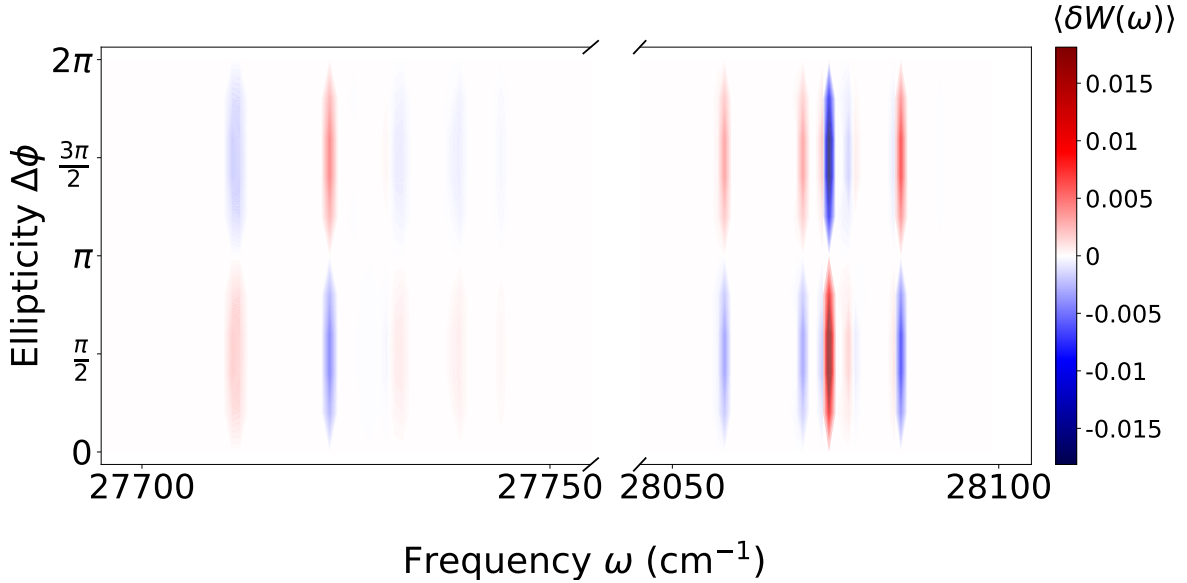


Figure 5: Computed circular dichroism (CD) spectrum for isotropic ensemble of molecular homotetramers under the influence of elliptically-polarized driving, where the CD signal  $\langle\delta W(\omega)\rangle$  is normalized with respect to the maximum absorption of the isotropic system when there is no laser-driving. Clear progressions of the CD as a function of ellipticity  $\Delta\phi$  can be observed, with sign switches at the time-reversal-symmetry (TRS) points  $\Delta\phi = 0, \pi$ . Note we have inserted a break in the frequency axes in order to highlight the CD signal about  $\omega_E$  and  $\omega_F$ .

## Conclusion

In this article, we have demonstrated that Floquet engineering with elliptically-polarized laser fields can serve as an alternative to magnetic fields to induce pseudo-MO effects in molecular systems and nanomaterials. These phenomena should be regarded as complementary to MCD and MOR effects in molecular systems. Small cyclic molecular aggregates with anisotropic arrangement of transition dipoles can support a wide range of excitonic AB phases upon elliptically polarized laser-driving despite the small areas they enclose. A rich ellipticity-dependent modulation of energy level splittings ensues, which concomitantly manifests in widely tunable CD spectra. Within the program of harnessing coherence in light-harvesting systems<sup>45–48</sup> and AB effects in quantum tunneling<sup>49</sup>, our study emphasizes the potential that AB phases have in the coherent control of energy and charge transport in molecular aggregates, as well as in the decongestion of spectra of the latter. While we have previously proposed the realization of excitonic AB phases in topologically protected porphyrin arrays<sup>23</sup>, such effects have been barely explored in a broader range of systems and they could be appealing as a way to switch exciton couplings and propagation direction on demand with lasers rather than by synthetic modification. Moreover, we have recognized that in the nanoscale, Floquet engineering is a dramatically less challenging tool than using magnetic fields to realize AB effects. In fact, the nanoscale excitonic AB phases that arise in our designed system depend on the pump laser ellipticity  $\Delta\phi$  and not on its field strength; thus a large phase of  $\Phi = \frac{\pi}{2}$  can in principle be readily realized in our protocol. This ease must be contrasted with the prohibitive magnetic fields that must be used in nanorings to induce an electronic AB phase of the same magnitude (we must mention, however, ingenious molecular electronics proposals to harness small AB phases arising from weak magnetic fields to induce substantial control on electronic currents<sup>50</sup>). Furthermore, it is important to emphasize that while general features of pseudo-MO and MO effects are similar (they both arise from breaking of TRS), they cannot be easily compared<sup>7</sup>: the former depends on coupling of time-varying electric fields with electric transition dipole moments, while the latter arises

from the interaction of static magnetic fields with the spin and orbital angular momentum of molecular eigenstates. Yet, we suspect that pseudo-MO effects could provide a convenient alternative in situations where magnetic fields are experimentally unfeasible.

The present article has laid the foundations of the generation of exciton AB phases in molecular aggregates. However, a detailed exploration of dissipative effects of a condensed phase environment must be addressed to ensure the experimental feasibility of our predictions in a wide range of experimental scenarios. Broadly speaking, we expect exciton AB phases to be resilient to decoherence as long as the light-matter coupling  $|\boldsymbol{\mu}_{LD} \cdot \mathbf{E}_{LD}(t)|$  and the excitonic couplings  $|J_{\alpha\beta}|$  are stronger than the spectral linewidths caused by the environment. These issues, together with the additional effects of intramolecular vibrations, will be addressed in future work.

*Note.* – After initial submission of the manuscript, we were made aware of an important reference by Phuc and Ishizaki<sup>26</sup>, which proposes Floquet engineering to control the chirality of electron transfer in molecular trimers. While the conclusions in that work are similar to the present, the AB phase in their work is due to linearly polarized light with two driving frequencies and amplitudes, rather than due to elliptically polarized light. While no isotropic averaging effects were discussed in that work, the authors carried out a thorough exploration of the effects of decoherence and concluded that chiral currents survive in the condensed phase. Further comparison of both strategies to induce AB phases will be the subject of future studies.

## Supplementary Information Available

Description of the Monte Carlo integration method used to calculate the CD for the driven homotetramer; presentation of the convergence of the CD signal calculation (Figure S1). This material is available free of charge via the Internet at <http://pubs.acs.org>.

## Acknowledgement

K.S. and J.Y.Z. acknowledge support from the Air Force Office of Scientific Research award FA9550-18-1-0289 for the excitonic design of AB phases and the Defense Advanced Research Projects Agency under Award No. D19AC00011 for the calculation of pseudo-MO effects. K.S. acknowledges discussions with R.F. Ribeiro, M. Du, and S. Pannir-sivajothi. Both authors acknowledge incisive and helpful comments by Reviewer 1.

## References

- (1) Barron, L. D. *Molecular Light Scattering and Optical Activity*; Cambridge University Press, 2009.
- (2) Lucarini, V.; Saarinen, J. J.; Peiponen, K.-E.; Vartiainen, E. M. *Kramers-Kronig Relations in Optical Materials Research*; Springer Science & Business Media, 2005; Vol. 110.
- (3) Thorne, J. Applications of the Faraday effect and magnetic circular dichroism in chemistry and physics. *Optical Polarimetry: Instrumentation and Applications*. 1977; pp 120–126.
- (4) Jones, R. M.; Inscore, F. E.; Hille, R.; Kirk, M. L. Freeze-quench magnetic circular dichroism spectroscopic study of the "very rapid" intermediate in xanthine oxidase. *Inorg. Chem.* **1999**, *38*, 4963–4970.
- (5) Ying, L.; Zhou, M.; Luo, X.; Liu, J.; Yu, Z. Strong magneto-optical response enabled by quantum two-level systems. *Optica* **2018**, *5*, 1156–1162.
- (6) Shoji, Y.; Mizumoto, T. Magneto-optical non-reciprocal devices in silicon photonics. *Sci. Technol. Adv. Mat.* **2014**, *15*, 014602.

- (7) Atkins, P.; Miller, M. Quantum field theory of optical birefringence phenomena: IV. The inverse and optical Faraday effects. *Mol. Phys.* **1968**, *15*, 503–514.
- (8) Aharonov, Y.; Bohm, D. Significance of electromagnetic potentials in the quantum theory. *Phys. Rev.* **1959**, *115*, 485.
- (9) Klitzing, K. v.; Dorda, G.; Pepper, M. New method for high-accuracy determination of the fine-structure constant based on quantized Hall resistance. *Phys. Rev. Lett.* **1980**, *45*, 494.
- (10) Ando, T.; Matsumoto, Y.; Uemura, Y. Theory of Hall effect in a two-dimensional electron system. *J. Phys. Soc. Jpn.* **1975**, *39*, 279–288.
- (11) Novoselov, K. S.; Jiang, Z.; Zhang, Y.; Morozov, S.; Stormer, H. L.; Zeitler, U.; Maan, J.; Boebinger, G.; Kim, P.; Geim, A. K. Room-temperature quantum Hall effect in graphene. *Science* **2007**, *315*, 1379–1379.
- (12) Tzuang, L. D.; Fang, K.; Nussenzeig, P.; Fan, S.; Lipson, M. Non-reciprocal phase shift induced by an effective magnetic flux for light. *Nat. Photonics* **2014**, *8*, 701.
- (13) Hafezi, M.; Mittal, S.; Fan, J.; Migdall, A.; Taylor, J. Imaging topological edge states in silicon photonics. *Nat. Photonics* **2013**, *7*, 1001.
- (14) Fang, K.; Yu, Z.; Fan, S. Realizing effective magnetic field for photons by controlling the phase of dynamic modulation. *Nat. Photonics* **2012**, *6*, 782.
- (15) Sigurdsson, H.; Kibis, O.; Shelykh, I. Optically induced Aharonov-Bohm effect in mesoscopic rings. *Phys. Rev. B* **2014**, *90*, 235413.
- (16) Kibis, O. V.; Sigurdsson, H.; Shelykh, I. A. Aharonov-Bohm effect for excitons in a semiconductor quantum ring dressed by circularly polarized light. *Phys. Rev. B* **2015**, *91*, 235308.

- (17) Kozin, V.; Iorsh, I.; Kibis, O.; Shelykh, I. Periodic array of quantum rings strongly coupled to circularly polarized light as a topological insulator. *Phys. Rev. B* **2018**, *97*, 035416.
- (18) Shirley, J. H. Solution of the Schrödinger equation with a Hamiltonian periodic in time. *Phys. Rev.* **1965**, *138*, B979.
- (19) Chu, S.-I. Generalized Floquet theoretical approaches to intense-field multiphoton and nonlinear optical processes. *Adv. Chem. Phys.* **1989**, *73*, 739–799.
- (20) Tannor, D. J. *Introduction to Quantum Mechanics: a Time-Dependent Perspective*; University Science Books, 2007.
- (21) Gu, B.; Franco, I. Optical absorption properties of laser-driven matter. *Phys. Rev. A* **2018**, *98*, 063412.
- (22) Maiuri, M.; Oviedo, M. B.; Dean, J. C.; Bishop, M.; Kudisch, B.; Toa, Z. S.; Wong, B. M.; McGill, S. A.; Scholes, G. D. High magnetic field detunes vibronic resonances in photosynthetic light harvesting. *J. Phys. Chem. Lett.* **2018**, *9*, 5548–5554.
- (23) Yuen-Zhou, J.; Saikin, S. K.; Yao, N. Y.; Aspuru-Guzik, A. Topologically protected excitons in porphyrin thin films. *Nat. Mater.* **2014**, *13*, 1026.
- (24) Oka, T.; Kitamura, S. Floquet engineering of quantum materials. *Annu. Rev. Condens. Ma. P.* **2019**, *10*, 387–408.
- (25) Thanh Phuc, N.; Ishizaki, A. Control of excitation energy transfer in condensed phase molecular systems by floquet engineering. *J. Phys. Chem. Lett.* **2018**, *9*, 1243–1248.
- (26) Phuc, N. T.; Ishizaki, A. Control of quantum dynamics of electron transfer in molecular loop structures: Spontaneous breaking of chiral symmetry under strong decoherence. *Phys. Rev. B* **2019**, *99*, 064301.

- (27) Römer, R. A.; Raikh, M. E. Aharonov-Bohm oscillations in the exciton luminescence from a semiconductor nanoring. *Phys. Status Solidi B* **2000**, *221*, 535–539.
- (28) Hu, H.; Zhu, J.-L.; Li, D.-J.; Xiong, J.-J. Aharonov-Bohm effect of excitons in nanorings. *Phys. Rev. B* **2001**, *63*, 195307.
- (29) Govorov, A.; Ulloa, S.; Karrai, K.; Warburton, R. Polarized excitons in nanorings and the optical Aharonov-Bohm effect. *Phys. Rev. B* **2002**, *66*, 081309.
- (30) Palmero, F.; Dorignac, J.; Eilbeck, J.; Römer, R. Aharonov-Bohm effect for an exciton in a finite-width nanoring. *Phys. Rev. B* **2005**, *72*, 075343.
- (31) Kuskovsky, I. L.; MacDonald, W.; Govorov, A.; Mourokh, L.; Wei, X.; Tamargo, M.; Tadic, M.; Peeters, F. Optical Aharonov-Bohm effect in stacked type-II quantum dots. *Phys. Rev. B* **2007**, *76*, 035342.
- (32) Lambert, W.; Felker, P.; Syage, J.; Zewail, A. Jet spectroscopy of anthracene and deuterated anthracenes. *J. Chem. Phys.* **1984**, *81*, 2195–2208.
- (33) Biggs, J. D.; Cina, J. A. Calculations of nonlinear wave-packet interferometry signals in the pump-probe limit as tests for vibrational control over electronic excitation transfer. *J. Chem. Phys.* **2009**, *131*, 224302.
- (34) Biggs, J. D.; Cina, J. A. Studies of impulsive vibrational influence on ultrafast electronic excitation transfer. *J. Phys. Chem. A* **2012**, *116*, 1683–1693.
- (35) Yamazaki, I.; Akimoto, S.; Aratani, N.; Osuka, A. Observation of coherent recurrence motion of excitons in anthracene dimers. *Bull. Chem. Soc. Jpn.* **2004**, *77*, 1959–1971.
- (36) Nitzan, A. *Chemical Dynamics in Condensed Phases: Relaxation, Transfer and Reactions in Condensed Molecular Systems*; Oxford university press, 2006.
- (37) Heller, E. J. *The Semiclassical Way to Dynamics and Spectroscopy*; Princeton University Press, 2018.



- (38) Maj, M.; Ahn, C.; Kossowska, D.; Park, K.; Kwak, K.; Han, H.; Cho, M.  $\beta$ -Isocyanoproline as an IR probe: comparison of vibrational dynamics between isonitrile and nitrile-derivatized IR probes. *Phys. Chem. Chem. Phys.* **2015**, *17*, 11770–11778.
- (39) Hofstadter, D. R. Energy levels and wave functions of Bloch electrons in rational and irrational magnetic fields. *Phys. Rev. B.* **1976**, *14*, 2239.
- (40) Baranowski, L. Equations of motion of a spin-stabilized projectile for flight stability testing. *J. Theor. App. Mech.* **2013**, *51*, 235–246.
- (41) Mukamel, S. *Principles of Nonlinear Optical Spectroscopy*; Oxford university press New York, 1995; Vol. 29.
- (42) Wilson, K. G. Confinement of quarks. *Phys. Rev. D* **1974**, *10*, 2445.
- (43) Stopkowicz, S.; Gauss, J.; Lange, K. K.; Tellgren, E. I.; Helgaker, T. Coupled-cluster theory for atoms and molecules in strong magnetic fields. *J. Chem. Phys.* **2015**, *143*, 074110.
- (44) Wang, Y.; Steinberg, H.; Jarillo-Herrero, P.; Gedik, N. Observation of Floquet-Bloch states on the surface of a topological insulator. *Science* **2013**, *342*, 453–457.
- (45) Scholes, G. D.; Fleming, G. R.; Chen, L. X.; Aspuru-Guzik, A.; Buchleitner, A.; Coker, D. F.; Engel, G. S.; Van Grondelle, R.; Ishizaki, A.; Jonas, D. M., et al. Using coherence to enhance function in chemical and biophysical systems. *Nature* **2017**, *543*, 647.
- (46) Calderón, L. F.; Pachón, L. A. Nonadiabatic Sunlight-harvesting. *arXiv preprint arXiv:1909.05029* **2019**,
- (47) Tiwari, V.; Peters, W. K.; Jonas, D. M. Electronic resonance with anticorrelated pigment vibrations drives photosynthetic energy transfer outside the adiabatic framework. *Proc. Natl. Acad. Sci. U.S.A.* **2013**, *110*, 1203–1208.

- (48) Chenu, A.; Christensson, N.; Kauffmann, H. F.; Mančal, T. Enhancement of vibronic and ground-state vibrational coherences in 2D spectra of photosynthetic complexes. *Sci. Rep.* **2013**, *3*, 2029.
- (49) Noguchi, A.; Shikano, Y.; Toyoda, K.; Urabe, S. Aharonov–Bohm effect in the tunnelling of a quantum rotor in a linear Paul trap. *Nat. Commun.* **2014**, *5*, 3868.
- (50) Hod, O.; Rabani, E.; Baer, R. Magnetoresistance of nanoscale molecular devices. *Accounts Chem. Res.* **2006**, *39*, 109–117.